Polymer 51 (2010) 5078–5086

Contents lists available at ScienceDirect

Polymer

journal homepage: www.elsevier.com/locate/polymer

Synthesis and property studies of linear and kinked poly(pyreneethynylene)s

Jhinuk Gupta, Sajini Vadukumpully, Suresh Valiyaveettil*

Department of Chemistry, National University of Singapore, 3 Science Drive 3, Singapore 117543

ARTICLE INFO

Article history:
Received 6 June 2010
Received in revised form
18 August 2010
Accepted 3 September 2010
Available online 15 September 2010

Keywords:
Conjugated polymer
Pyrene
Polymer synthesis

ABSTRACT

A series of fluorescent conjugated polymers, poly(pyreneethynylene)s, have been designed and synthesized to investigate the effect of shape of polymer backbone on physical properties. Polymers with linear and kinked backbone were synthesized using 1,6- and 1,8-disubstituted pyrene. The target copolymers were designed to incorporate various spacer units, such as, alkoxyphenyl, carbazole and fluorene on the polymer backbone. Characterization of the target compounds was achieved by NMR, IR, GPC and MALDI-TOF mass spectrometry. Detailed investigation on their optical, electrochemical and thermal properties revealed significant contribution of the geometry of polymer backbone towards physical properties. Kinked backbone of *cisoid*-polymers was found to result in lower optical band gap, less negative E_{HOMO} and higher thermal stability as compared to their linear analogues, most probably due to the coiling of polymer chains. Comparison of the physical properties of the polymers with those of the model compounds suggested similar extent of conjugation through 1,6- and 1,8-position of pyrene.

1. Introduction

Synthesis of structurally versatile π-conjugated polymers is interesting owing to their extensive use in technologies such as LED displays [1–6], molecular electronics [7–11], sensors [12,13] and lasers [14]. Developing new fluorescent polymers with interesting properties, such as, higher quantum efficiency, charge transfer mobility, thermal stability, solubility and ease of processiblity allows us to explore interesting applications. All these physical properties can be manipulated through proper molecular design. Poly(phenyleneethynylene) is one of the well explored class of fluorescent conjugated polymers [15]. Structure–property relationship of homopolymers [16] and copolymers [17,18] of poly(*p*-phenyleneethynylene) is reported in literature. Chemical nature and shape of backbone influence the physical properties of polymers. It is found that introduction of kinks or twists on the polymer chain reduces the stiffness and enhances the processibility. For example, incorporation of 2,5-thienylene [19] and *m*-phenylene [18] groups in poly(*p*-phenyleneethynylene) systems enhances the flexibility and processibility of the resulting polymers by introducing a twist of 143° and 120° to the polymer backbone. Pyrene may be considered as a rigid unit to influence the backbone and enhance the fluorescence properties. Pyrene is one of the interesting fluorophores to show high quantum yield, longer fluorescence life time, high thermal stability and significant π-stacking ability in solution or solid state. Moreover, pyrene offers the possibility of incorporating interesting structural features to the polymer backbone due to easy functionalization at various positions. It is conceivable that selective functionalization of pyrene at 1,8-positions (*cis*) introduces a kink of 63° on the polymer backbone whereas, functionalization at 1,6-positions (*trans*) gives a linear polymer. Polymers with pendant pyrene moieties are common [20–22], but, only a few polymers and oligomers with pyrene incorporated on the polymer backbone are known in literature [23–25].

In this work, synthesis and characterization of a series of conjugated poly(pyreneethynylene)s are reported, where diethynylpyrene is copolymerized with various spacer units, such as alkoxybenzene, carbazole and fluorene (Fig. 1). The shapes of the polymer backbones are controlled by using 1,6- and 1,8-disubstitution on the pyrene moieties. Synthesized polymers are named as *cisoid*-(**1**, **3**, **5**) or *transoid*-(**2**, **4**, **6**) depending on different mode of functionalization (1,8- *vs.* 1,6-) on pyrene. Unlike the reported phenylene based systems [16,18], both *cisoid* and *transoid* have strong π-conjugation. Thus the system allows us to investigate solely the effect of shape on the properties of the polymers. In addition, two structurally related model compounds (**7** and **8**) are designed for comparison purpose.

2. Experimental section

2.1. Materials and methods

All reagents were purchased from commercial sources and used without further purification unless otherwise stated. Tetrahydrofuran

---

* Corresponding author. Tel.: +65 65164327; fax: +65 67791691.
E-mail address: chmsv@nus.edu.sg (S. Valiyaveettil).

0032-3861/$ – see front matter © 2010 Elsevier Ltd. All rights reserved.
doi:10.1016/j.polymer.2010.09.012

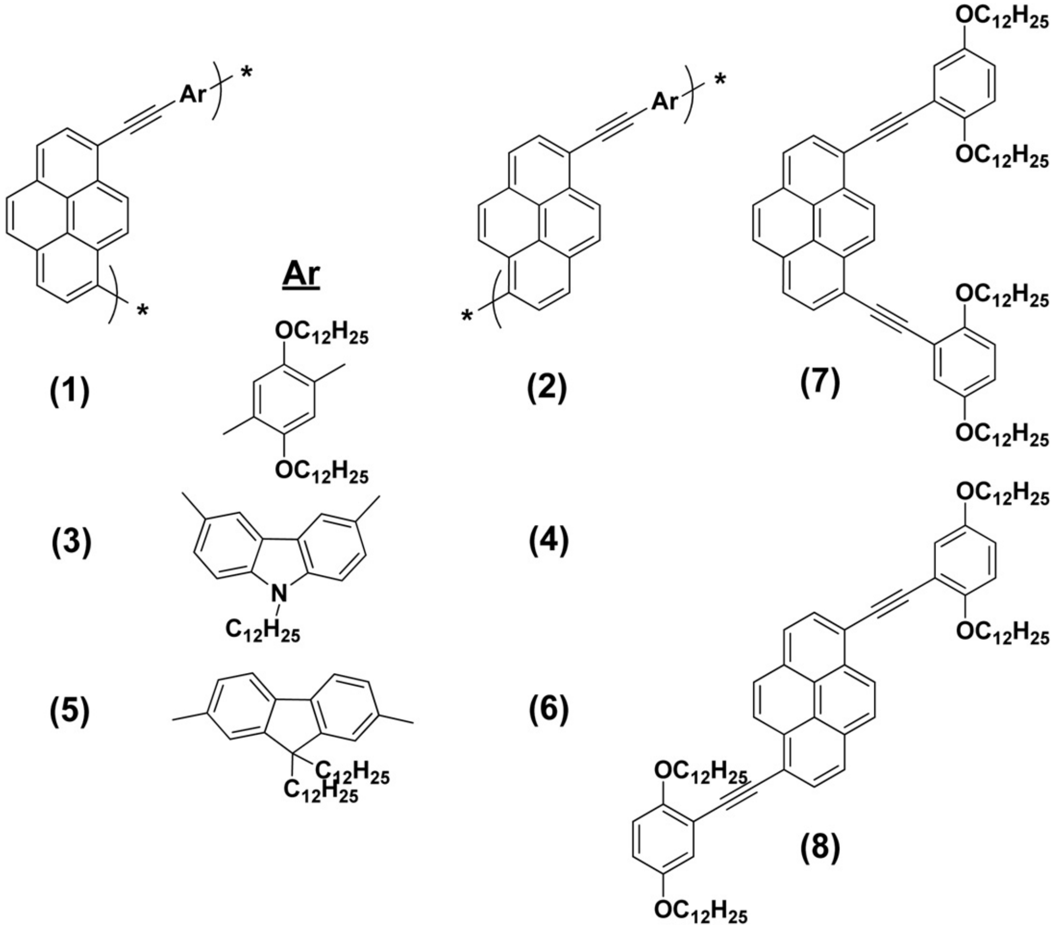

Fig. 1. Structure of the target compounds.

(THF) was purified by distillation over sodium under nitrogen atmosphere. The ^{1}H and ^{13}C NMR spectra were collected on a Bruker ACF 300 spectrometer operating at 300 and 75.5 MHz, respectively. $CDCl_3$ was used as solvent with tetramethylsilane as internal standard. FT-IR spectra were recorded using BIO-RAD FT-IR spectrophotometer. MALDI-TOF mass spectra of the compounds were recorded using Bruker Deltronix Autoflex II instrument. Solution of 1,8,9-trihydroxyanthracene (0.1 M) and 2,5-dihydroxybenzoic acid (0.1 M) in THF was used to prepare the matrix. Molecular weight of the polymers was determined using Shimadzu LC vt 10AT gel permeation chromatography (GPC) instrument equipped with UV and refractive index (RI) detectors connected in series, polystyrene as standard and THF as an eluent at a flow rate of 0.3 mL/min. UV–vis spectra were recorded using a Shimadzu 3101 PC spectrophotometer and fluorescence measurements were made on an RF-5301PC Shimadzu spectrofluorophotometer. The quantum yields of the synthesized compounds in dichloromethane (DCM) were measured using quinine sulfate (0.1 M H_2SO_4) as a reference [26]. The chromaticity of the compounds was measured using chromameter CS 100 A. The electrochemical behavior of the compounds was investigated with cyclic voltammetry (CV). CV experiments were performed using an Autolab potentiostat (model PGSTAT30) by Echochimie and data recorded in acetonitrile with 0.1 M tetrabutylammonium hexafluorophosphate as supporting electrolyte (scan rate of 100 mV s^{-1}). The experiments were performed at room temperature with a conventional three-electrode configuration consisting of an indium tin oxide (ITO) working electrode, a platinum counter electrode, and Hg/Hg_2Cl_2 in 3 M KCl as reference electrode. Thermogravimetric analyses (TGA) were done on a TA-SDT 2960 at a heating rate of 10 °C/min under nitrogen atmosphere. Differential scanning calorimetry (DSC) thermograms were recorded using a TA-DSC 2920 at a heating rate of 10 °C/min under nitrogen atmosphere. Scanning electron microscopic (SEM) images were recorded in JEOL JEM-6010 F field emission scanning electron microscope. Atomic force microscopy (AFM) experiment was performed at room temperature using a commercial AFM Nanoscope IV (Dimension 3100, Digital Instruments) in the tapping mode. The samples for SEM and AFM experiments were prepared by evaporating a few drops of toluene solution of the polymers on glass plates and clean ITO substrates, respectively.

2.2. *Synthesis*

Compounds **11** [27,28], **13** [29], **15** [30], **16a**, **16b** [31], **17a**, **17b**, **18a** and **18b** [32,33] were prepared using reported procedures.

2.2.1. *General synthetic procedure for Sonogashira polymerization*

To a degassed solution of freshly distilled THF and triethylamine, dihalocompound (**11** or **13** or **15**), CuI, PPh_3 and $Pd(PPh_3)_2Cl_2$ were added under nitrogen atmosphere. The terminal acetylene was added to the stirred solution at 55 °C (for **11**) or 80 °C (for **13** and **15**) and the heating was continued for 5 days under nitrogen atmosphere. After cooling, the reaction mixture was added dropwise to a methanol/water mixture (98:2). The precipitated polymer was filtered and purified by reprecipitation from methanol.

*2.2.1.1. Synthesis of polymer **1**.* Compound **11** (560 mg, 0.80 mmol), $Pd(PPh_3)_2Cl_2$ (28 mg, 0.04 mmol), CuI (16 mg, 0.08 mmol), PPh_3 (42 mg, 0.16 mmol), **18a** (200 mg, 0.80 mmol), triethylamine (15 mL), THF (30 mL). Yield = 300 mg, 40%.

^{1}H NMR (300 MHz, $CDCl_3$, ppm) δ: 8.98–8.08 (pyrene and phenyl $\underline{H}$s), 4.22 ($-O-C\underline{H}_2-$), 4.10 ($-O-C\underline{H}_2-$), 2.08–0.77 (alkyl $\underline{H}$s). ^{13}C NMR (75.5 MHz, $CDCl_3$, ppm) δ: 153.8, 132.3, 131.4, 130.7, 129.7, 128.8, 127.8, 126.7, 125.1, 124.3, 118.8, 116.4, 115.8, 114.2 (pyrene and phenyl $-\underline{C}H-$), 94.6, 92.8 ($-\underline{C}\equiv\underline{C}-$), 69.6, 68.1, 38.9, 32.0, 29.8, 29.4, 26.4, 23.8, 22.7, 14.2, 10.7. FT-IR (KBr, cm^{-1}): 2923, 2849, 2364, 2200, 1596, 1562, 1511, 1465, 1380, 1278, 1215, 1032, 850, 724.

*2.2.1.2. Synthesis of polymer **2**.* Compound **11** (392 mg, 0.56 mmol), $Pd(PPh_3)_2Cl_2$ (20 mg, 0.03 mmol), CuI (12 mg, 0.06 mmol), PPh_3 (30 mg, 0.12 mmol), **18b** (138 mg, 0.56 mmol), triethylamine (10 mL), THF (20 mL). Yield = 350 mg, 66%.

^{1}H NMR (300 MHz, $CDCl_3$, ppm) δ: 8.89–7.87 (pyrene and phenyl $\underline{H}$s), 4.22–3.92 ($-O-C\underline{H}_2-$), 1.58–0.86 (alkyl $\underline{H}$s). ^{13}C NMR (75.5 MHz, $CDCl_3$, ppm) δ: 154.0, 132.0, 130.9, 129.6, 128.8, 127.9, 126.8, 125.0, 124.2, 118.9, 116.3, 115.8, 114.2, 113.8 (pyrene and phenyl $-\underline{C}H-$), 94.6, 92.6 ($-\underline{C}\equiv\underline{C}-$), 69.6, 68.2, 38.8, 31.9, 29.7, 29.3, 26.4, 26.3, 26.1, 22.6, 14.1, 10.7. FT-IR (KBr, cm^{-1}): 2974, 2923, 2854, 2354, 2205, 1727, 1465, 1271, 1209, 845.

*2.2.1.3. Synthesis of polymer **3**.* Compound **13** (986 mg, 2.00 mmol), $Pd(PPh_3)_2Cl_2$ (70 mg, 0.10 mmol), CuI (38 mg, 0.20 mmol), PPh_3 (105 mg, 0.40 mmol), **18a** (500 mg, 2.00 mmol), triethylamine (30 mL), THF (60 mL). Yield = 680 mg, 30%.

^{1}H NMR (300 MHz, $CDCl_3$, ppm) δ: 8.86–7.39 (pyrene and carbazole $\underline{H}$s), 4.24–4.19 ($-N-C\underline{H}_2-$), 1.83–0.87 (alkyl $\underline{H}$s). ^{13}C NMR (75.5 MHz, $CDCl_3$, ppm) δ: 140.4, 139.3, 131.7, 130.0, 129.7, 129.0, 128.8, 128.6, 128.5, 128.4, 127.7, 127.6, 126.4, 126.3, 125.0, 124.3, 124.2, 123.4, 123.3, 123.2, 122.0, 121.9, 119.0, 114.0, 112.2, 111.9, 110.4, 109.1 (pyrene and carbazole $-\underline{C}H-$), 96.9, 87.2 ($-\underline{C}\equiv\underline{C}-$), 43.3, 31.9, 29.6, 29.51, 29.47, 29.43, 29.3, 28.8, 27.2, 27.1, 22.7, 14.1. FT-IR (KBr, cm^{-1}): 3488, 3427, 2916, 2854, 2191, 1878, 1589, 1466, 1357, 1281, 1217, 1141, 1048, 849, 801, 711.

*2.2.1.4. Synthesis of polymer **4**.* Compound **13** (315 mg, 0.64 mmol), $Pd(PPh_3)_2Cl_2$ (23 mg, 0.03 mmol), CuI (13 mg, 0.06 mmol), PPh_3 (34 mg, 0.13 mmol), **18b** (160 mg, 0.64 mmol), triethylamine (25 mL), THF (50 mL). Yield = 230 mg, 48%.

^{1}H NMR (300 MHz, $CDCl_3$, ppm) δ: 8.79–7.43 (pyrene and carbazole $\underline{H}$s), 4.30–4.21 ($-N-C\underline{H}_2-$), 1.82–0.85 (alkyl $\underline{H}$s). ^{13}C NMR (75.5 MHz, $CDCl_3$, ppm) δ: 139.4, 139.3, 131.7, 131.1, 130.0, 129.8, 129.0, 128.8, 128.5, 128.4, 127.6, 126.4, 125.0, 124.2, 123.4, 123.2, 122.0, 119.0, 114.0, 112.2, 111.9, 110.4, 109.1 (pyrene and carbazole $-\underline{C}H-$), 96.9, 87.2 ($-\underline{C}\equiv\underline{C}-$), 43.3, 31.9, 29.6, 29.51, 29.47, 29.4, 29.3, 28.9, 28.8, 27.21, 27.19, 22.6, 14.1. FT-IR (KBr, cm^{-1}): 3443, 3038, 2918, 2855, 2191, 1887, 1589, 1481, 1358, 1280, 1220, 1142, 1064, 956, 849, 724.

*2.2.1.5. Synthesis of polymer **5**.* Compound **15** (660 mg, 1.00 mmol), $Pd(PPh_3)_2Cl_2$ (35 mg, 0.05 mmol), CuI (19 mg, 0.10 mmol), PPh_3 (52 mg, 0.20 mmol), **18a** (250 mg, 1.00 mmol), triethylamine (30 mL), THF (60 mL). Yield = 530 mg, 58%.

^{1}H NMR (300 MHz, $CDCl_3$, ppm) δ: 8.91–7.44 (pyrene and fluorene $\underline{H}$s), 2.12–0.82 (alkyl $\underline{H}$s). ^{13}C NMR (75.5 MHz, $CDCl_3$, ppm) δ: 153.3, 152.6, 151.4, 150.6, 141.0, 140.6, 139.4, 139.0, 131.9, 131.8, 131.4, 131.1, 130.2, 130.0, 128.5, 128.0, 126.5, 126.2, 126.0, 125.2, 124.3, 122.2, 121.7, 121.4, 121.1, 120.2, 119.9, 118.7 (pyrene and fluorene $-\underline{C}H-$), 96.7, 89.0 ($-\underline{C}\equiv\underline{C}-$), 55.6, 53.4, 40.3, 40.1, 31.9, 30.0, 29.6, 29.3, 23.8, 23.6, 22.6, 14.1. FT-IR (KBr, cm^{-1}): 3429, 3037, 2917, 2855, 2191, 1878, 1589, 1451, 1249, 1189, 1110, 1065, 1003, 833, 710.

*2.2.1.6. Synthesis of polymer **6**.* Compound **15** (423 mg, 0.64 mmol), $Pd(PPh_3)_2Cl_2$ (23 mg, 0.03 mmol), CuI (13 mg, 0.06 mmol), PPh_3 (34 mg, 0.13 mmol), **18b** (160 mg, 0.64 mmol), triethylamine (25 mL), THF (50 mL). Yield = 310 mg, 53%.

^{1}H NMR (300 MHz, $CDCl_3$, ppm) δ: 8.80–7.43 (pyrene and fluorene $\underline{H}$s), 2.03–0.66 (alkyl $\underline{H}$s). ^{13}C NMR (75.5 MHz, $CDCl_3$, ppm) δ: 153.3, 151.4, 150.6, 141.0, 139.5, 132.0, 131.9, 131.7, 131.2, 131.0, 130.1, 130.0, 128.5, 128.4, 128.2, 126.3, 126.0, 125.6, 125.2, 124.3, 122.1, 121.7, 121.4, 120.2, 119.9, 118.7 (pyrene and fluorene $-\underline{C}H-$), 96.8, 89.1 ($-\underline{C}\equiv\underline{C}-$), 55.6, 55.5, 53.4, 40.3, 40.1, 31.9, 30.1, 30.0, 29.6, 29.3, 23.8, 22.7, 14.1 ($-\underline{C}H_2$). FT-IR (KBr, cm^{-1}): 3426, 3037, 2916, 2855, 2191, 1887, 1605, 1466, 1252, 1187, 1065, 1002, 895, 834, 726.

*2.2.2. Synthesis of compound **10***

Compound **9** (380 mg, 0.85 mmol), KIO_3 (36 mg, 0.17 mmol) and I_2 (119 mg, 0.47 mmol) were added to a mixture of acetic acid (10 mL), H_2SO_4 (0.1 mL) and water (1 mL). The mixture was gradually brought to reflux and continued refluxing for 6 h. After cooling the reaction mixture to room temperature, the unreacted iodine was quenched using 20% aqueous $Na_2S_2O_3$. The precipitate was collected and washed with water. The air-dried solid was purified by column chromatography using hexane as the eluent. The pure compound was obtained as colorless semisolid with 32% yield (156 mg).

^{1}H NMR (300 MHz, $CDCl_3$, ppm) δ: 7.32 (1H, d, $J = 2.94$ Hz, $I-C-C\underline{H}$), 6.83 (1H, dd, $J = 2.94$ Hz and 8.88 Hz, $I-C\text{-}C-CO-C\underline{H}-$), 6.72 (1H, d, $J = 8.88$ Hz, $I-C-CO-C\underline{H}-$), 3.93 (2H, t, $-O-C\underline{H}_2-$), 3.87 (2H, t, $-O-C\underline{H}_2-$), 1.84–0.90 (40H, m, alkyl $\underline{H}$s), 0.88 (6H, t, $-C\underline{H}_3$). ^{13}C NMR (75.5 MHz, $CDCl_3$, ppm) δ: 153.8 ($-O-\underline{C}-CH-$), 152.2 ($-O-\underline{C}-CH-$), 125.4 ($-\underline{C}H-$), 115.4 ($-\underline{C}H-$), 113.1 ($-\underline{C}H-$), 87.0 ($I-\underline{C}-CH-$), 70.2 ($-O-\underline{C}H_2-$), 68.8 ($-O-\underline{C}H_2-$), 31.9, 29.6, 29.5, 29.3, 29.2, 26.1, 26.0, 22.7, 14.1 (alkyl $\underline{C}$s).

2.2.3. General synthetic procedure for Sonogashira coupling reaction

To a degassed solution of freshly distilled THF and triethylamine, **10**, CuI, PPh_3 and $Pd(PPh_3)_2Cl_2$ were added under a continuous nitrogen flow. Diethynylpyrene (**18a** or **18b**) was added to the stirred solution at 55 °C and the heating was continued for 24 h under nitrogen atmosphere. The solvent was removed completely under vacuum to get the crude product which was purified through column chromatography.

*2.2.3.1. Synthesis of compound **7**.* Compound **10** (189 mg, 0.33 mmol), $Pd(PPh_3)_2Cl_2$ (5 mg, 0.01 mmol), CuI (3 mg, 0.01 mmol), PPh_3 (8 mg, 0.03 mmol), triethylamine (10 mL), THF (20 mL), **18a** (33 mg, 0.13 mmol). Column chromatography using 4:1 hexane/DCM. Yield = 92 mg, 61%.

^{1}H NMR (300 MHz, $CDCl_3$, ppm) δ: 8.93 (2H, s, pyrene $-C\underline{H}-$), 8.23–8.04 (6H, m, pyrene $-C\underline{H}-$), 7.22 (2H, s, phenyl $-C\underline{H}-$), 6.90 (4H, s, phenyl $-C\underline{H}-$), 4.11 (4H, t, $-O-C\underline{H}_2-$), 3.98 (4H, t, $-O-C\underline{H}_2-$), 2.03–1.07 (80H, m, alkyl $\underline{H}$s), 0.92–0.83 (12H, m, $-C\underline{H}_3$). ^{13}C NMR (75.5 MHz, $CDCl_3$, ppm) δ: 154.4 ($-O-\underline{C}-CH-$), 152.9 ($-O-\underline{C}-CH-$), 132.0, 131.2, 129.7, 127.8, 126.7, 124.9, 124.2, 119.0, 118.4, 116.5, 113.8, 113.6 (pyrene and phenyl $-\underline{C}H-$), 92.6, 92.4 ($-\underline{C}\equiv\underline{C}-$), 69.7, 68.8 ($-O-\underline{C}H_2-$) 31.9, 31.8, 29.69, 29.64, 29.55, 29.53, 29.46, 29.42, 29.36, 29.3, 26.3, 26.1, 22.7, 22.6, 14.1 (alkyl $\underline{C}$s). FT-IR (KBr, cm^{-1}): 2955, 2921, 2854, 2363, 2336, 2196, 1644, 1488, 1466, 1377, 1304, 1276, 1220, 1159, 1026, 853, 797, 758, 724. MALDI-TOF MS: Calcd. for $C_{80}H_{114}O_4$: 1140. Found: 1141 $[M+H]^+$.

*2.2.3.2. Synthesis of compound **8**.* Compound **10** (189 mg, 0.33 mmol), $Pd(PPh_3)_2Cl_2$ (5 mg, 0.01 mmol), CuI (3 mg, 0.01 mmol), PPh_3 (8 mg, 0.03 mmol), triethylamine (10 mL), THF (20 mL), **18b** (33 mg,

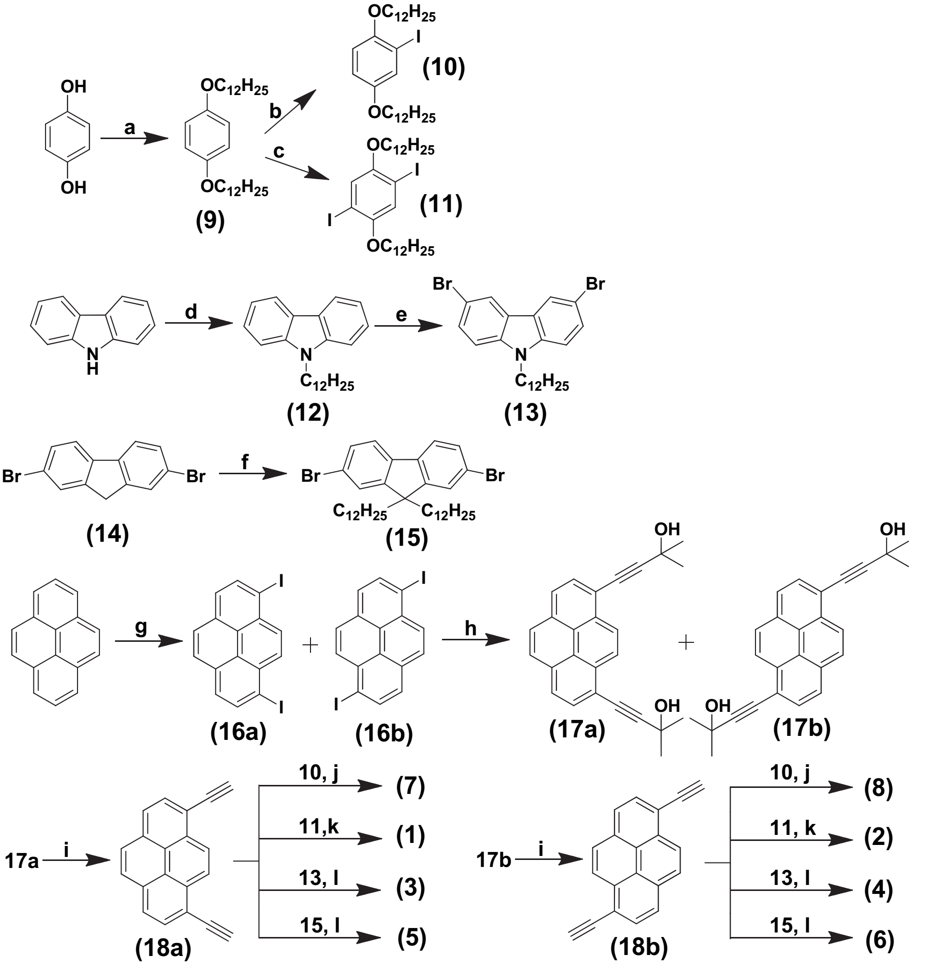

Scheme 1. Synthesis of the target compounds: (a) K_2CO_3, acetone, 1-dodecylbromide, N_2, reflux, 3 d; (b) I_2/KIO_3, HOAc, H_2SO_4, H_2O, room temperature to reflux, 6 h; (c) I_2/KIO_3, HOAc, H_2SO_4, H_2O, reflux, 6 h; (d) Tetrabutylammonium bromide, 50% NaOH, 1-bromododecane, toluene, 70 °C, 24 h; (e) NBS, dichloromethane, 0 °C to room temperature, 6 h; (f) Triethylbenzylammonium chloride, 1-bromododecane, 50% NaOH, 60 °C, 12 h; (g) I_2/KIO_3, HOAc, H_2SO_4, H_2O, 40 °C, 4 h; (h) 2-Methylbut-3-yn-2-ol, Et_3N, $Pd(PPh_3)_2Cl_2$, CuI, 50 °C, 20 h; (i) NaOH, toluene, reflux, 3 h; (j) THF, Et_3N, $Pd(PPh_3)_2Cl_2$, CuI, PPh_3, 55 °C, 24 h; (k) THF, Et_3N, $Pd(PPh_3)_2Cl_2$, CuI, PPh_3, 55 °C, 5 d; (l) THF, Et_3N, $Pd(PPh_3)_2Cl_2$, CuI, PPh_3, 80 °C, 5 d.

0.13 mmol). Column chromatography using 82:18 hexane/DCM. Yield = 106 mg, 70%.

^1H NMR (300 MHz, $CDCl_3$, ppm) δ: 8.86 (2H, d, J = 9.03 Hz, pyrene $-C\underline{H}-$), 8.22−8.11 (6H, m, pyrene $-C\underline{H}-$), 7.20 (2H, s, phenyl $-C\underline{H}-$), 6.90 (4H, d, J = 1.32, phenyl $-C\underline{H}-$), 4.12 (4H, t, $-O-C\underline{H_2}-$), 3.98 (4H, t, $-O-C\underline{H_2}-$), 2.05−1.17 (80H, m, alkyl $\underline{H}$s), 0.90−0.82 (12H, m, $-C\underline{H_3}$). ^{13}C NMR (75.5 MHz, $CDCl_3$, ppm) δ: 154.4 ($-O-\underline{C}-CH-$), 152.8 ($-O-\underline{C}-CH-$), 132.2, 131.1, 129.6, 127.9, 126.7, 125.0, 124.3, 118.9, 118.4, 116.6, 113.6, 113.4 (pyrene and phenyl $-\underline{C}H-$), 92.6, 92.3 ($-\underline{C}\equiv\underline{C}-$), 69.6, 68.8, 31.9, 31.8, 29.6, 29.43, 29.40, 29.35, 29.32, 26.2, 26.1, 22.68,22.66, 14.1 (alkyl $\underline{C}$s). FT-IR (KBr, cm^{-1}): 2957, 2917, 2849, 2359, 2335, 2205, 1602, 1505, 1471,1408, 1397, 1323, 1289, 1272, 1221, 1164, 1146, 1044, 1026, 850, 816, 776, 719. MALDI-TOF MS: Calcd. for $C_{80}H_{114}O_4$: 1140. Found: 1141 $[M + H]^+$.

3. Results

3.1. Synthesis and characterization

Syntheses of the target compounds are illustrated in Scheme 1. 1,8- or 1,6-Diethynylpyrene (**18**) was polymerized with dihaloderivatives of phenyl, carbazole and fluorene under Sonogashira coupling conditions. Dihaloderivatives were synthesized following reported procedures with or without modifications. Diiodination of pyrene, followed by coupling with 2-methylbut-3-yn-2-ol generated the mixture of **17a** and **17b**. These two isomers were separated owing to high degree of intermolecular H-bonding in **17b**, which allowed it to precipitate out immediately from a DCM solution. Terminal acetylene groups were deprotected using sodium hydroxide in boiling toluene. Coupling of **18a** and **18b** to **11**, **13** and **15** generated the series of target polymers. Compounds **18a** and **18b** were coupled to the monoiododerivative **10** to synthesize two model compounds **7** and **8**. All polymers were red in colour, whereas, oligomers were yellow in colour. Solubility of the synthesized compounds were checked in common organic solvents, e.g. cyclohexane, DCM, chloroform, THF, acetonitrile and dimethylsulfoxide, with the compounds showing maximum solubility in DCM, chloroform and THF. In general, *cisoid*-polymers (**1**, **3** and **5**) were more soluble as compared to their *transoid*-counter parts (**2**, **4** and **6**).

Full characterization of the compounds was accomplished with NMR, IR and MALDI-TOF mass spectrometry and GPC. Though ^1H NMR spectra of the polymers were not well resolved as compared to the model compounds, the regions for characteristic peaks could be identified. NMR signals of aromatic protons of pyrene and associated phenyl/carbazole/fluorene units appeared between 8.9 and 7.4 ppm. Signal for alkyl protons were observed between 2.0

Table 1
Molecular weight and TGA data of the target compounds.

Polymer	M_{w}[a]	M_{n}[a]	PDI[a]	T_5[b] (°C)
1	18,700	11,900	1.6	234
2	12,400	9800	1.3	222
3	12,600	9000	1.4	300
4	11,600	8400	1.4	277
5	11,900	8600	1.3	329
6	12,300	8200	1.5	310
7	–	1141[c]	–	338
8	–	1141[c]	–	344

[a] Determined by GPC using polystyrene standard.
[b] Temperature corresponding to 5% weight loss.
[c] $[M+H]^+$ determined by MALDI-TOF mass spectrometry.

and 0.8 ppm, whereas, alkyl protons connected to oxygen or nitrogen atoms shifted to a lower field (4.3–3.9 ppm). GPC was used to estimate the molecular weight of the polymers. Weight average (M_{w}) and number average (M_{n}) molecular weights along with polydispersity index (PDI) are listed in Table 1.

3.2. Thermal properties

Thermogravimetric analyses were done for all target compounds. The detailed findings are listed in Table 1. All polymers showed similar trend in thermal properties with one sharp decomposition followed by gradual decay (Fig. 2a). Some residual weight remained even beyond 900 °C indicating char formation. The first decomposition of polymers signifies partial or complete breaking of alkyl chains from polymer backbone. Model compounds (**7** and **8**) showed sharp single step decomposition (Fig. 2b).

Thermal properties of polymers were examined between −40 °C and decomposition temperature (~220–300 °C) using a differential scanning calorimetry (DSC). DSC traces of the polymers did not show any glass transition or melting before degradation. This property is quite similar with poly(phenyleneethynylene)s [15] and can be attributed to the curing reaction between acetylene groups on the polymer backbone during heating [34]. DSC trace (Fig. 2c) of the model compound **7** showed three phase transitions at 45 °C (12.6 kJ mol^{-1}), 75 °C (42.1 kJ mol^{-1}) and 100 °C (49.5 kJ mol^{-1}). Compound **7** melts to a discotic phase at 75 °C, followed by isotropization at 100 °C. The cooling trace exhibited isotropic–discotic transition at 63 °C followed by crystallization at 42 °C [35]. The liquid crystalline nature of **7** indicated by DSC trace was further examined using polarized optical microscope (Supplementary material Fig. S13). Compound **8**, with a single phase transition (112 °C, 161.2 kJ mol^{-1}) between crystal and isotropic phases, did not show any liquid crystalline phase (Fig. 2d).

3.3. Optical properties

Optical property is useful to gain information regarding structure–property relationship of compounds. Detailed study of optical properties of all target compounds was accomplished in solution and in thin film (Figs. 3 and 4), the results are summarized in Table 2. It is observed that all polymers and oligomers have more than one strong absorption and emission peaks, which is a characteristic feature of a pyrene moiety [36].

Enhanced conjugation offered by ethynyl bonds shift the absorption wavelengths of both polymers and model compounds to red region ($\lambda_{\mathrm{abs}} = 450–500$) as compared to pyrene ($\lambda_{\mathrm{abs}} = 335$ nm) and the previously reported poly(pyrenevinyl) system ($\lambda_{\mathrm{abs}} = 395$ nm) [24]. Optical properties of target compounds were examined in different solvents and no significant polarity dependance was detected. Similar absorption–emission spectra were observed in cyclohexane, DCM and acetonitrile. All synthesized compounds showed Stokes shift in the range of 15–30 nm which could be due to mechanisms such as intersystem crossing, migration of excitons along the polymer chains and configurational relaxation of excited states, as reported by other research groups working on similar

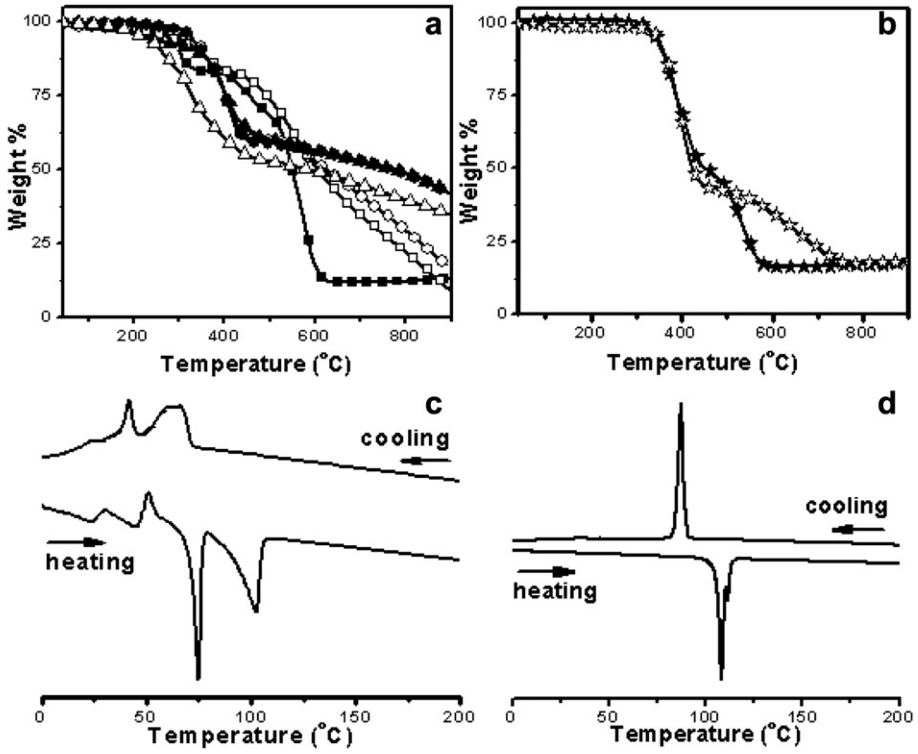

Fig. 2. Thermograms of polymers (a) and model compounds (b). **1** (▲) **2** (△) **3** (■) **4** (□) **5** (●) **6** (○) **7** (★) **8** (☆). DSC traces of (c) **7** and (d) **8**.

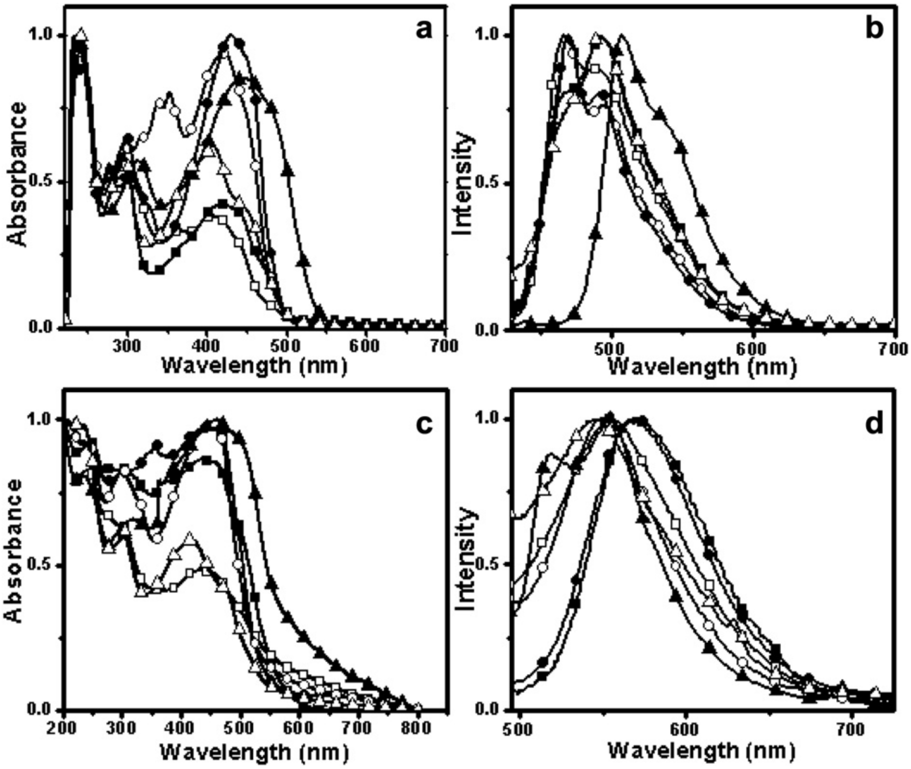

Fig. 3. Absorption (a, c) and emission (b, d) spectra of the polymers in DCM (0.1 mg/mL, 28 °C) (a, b) and thin film (c, d). **1** (▲) **2** (△) **3** (■) **4** (□) **5** (●) **6** (○).

polymers [16,37,38]. Identification of the exact mechanism is currently in progress and will be reported elsewhere.

Fluorescence quantum yields were measured for the compounds using quinine sulfate as standard. Autoquenching of fluorescence results in much lower quantum yield for the polymers as compared to the model compounds (**7** and **8**). Amongst various polymers, *transoid*-series (**2**, **4**, **6**) showed higher quantum yield as compared to their *cisoid*-(**1**, **3**, **5**) analogues. Thin films of polymers and model

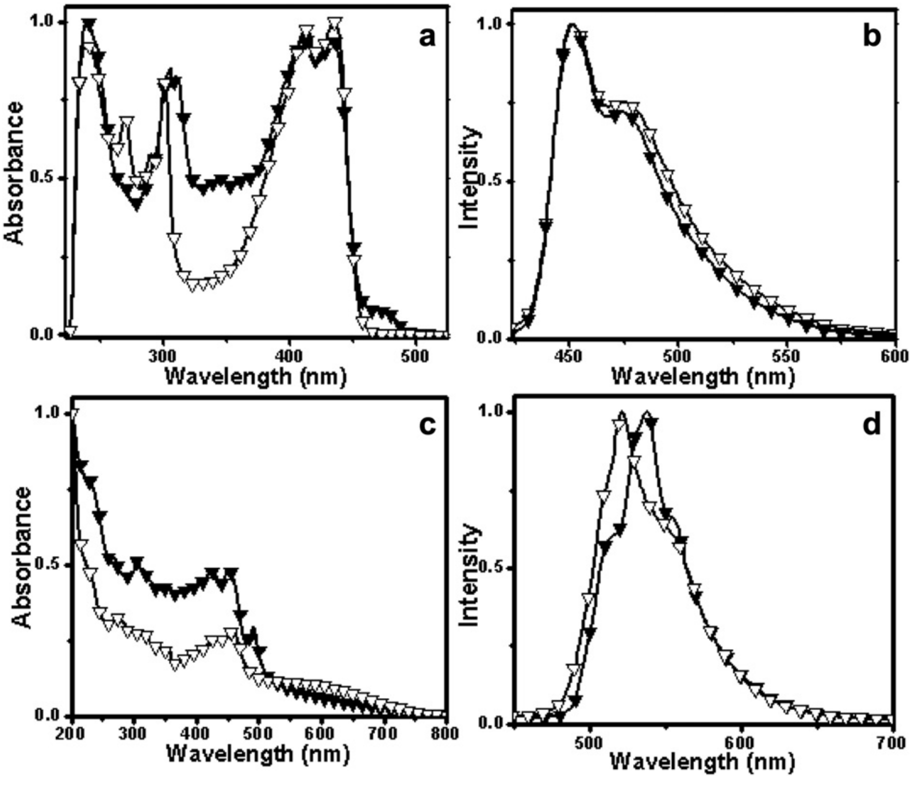

Fig. 4. Absorption (a, c) and emission (b, d) spectra of model compound **7** (▼) and **8** (▽) in DCM (10^{-5} M, 28 °C) (a, b) and thin film (c, d).

Table 2
Optical properties of the target compounds.

Compound	Solution[a]						Film[b]	
	λ_{abs} (nm)	λ_{em} (nm)	Band gap[c] (eV)	Quantum yield	Stokes shift (nm)	CIE coordinates[d]	λ_{abs} (nm)	λ_{em} (nm)
1	484, 446, 313	544, 508	2.30	0.18	24	0.420, 0.437	502, 460, 322	554, 518
2	450, 407, 295	493, 467	2.43	0.20	17	0.404, 0.420	477, 419, 299	546
3	473, 418, 294	494, 470	2.44	0.14	21	0.413, 0.430	505, 434, 306	571
4	441, 407, 306	494, 467	2.58	0.20	26	0.407, 0.422	500, 430, 307	555
5	453, 430, 299	493, 470	2.53	0.17	17	0.408, 0.431	450	571
6	452, 419, 353	497, 470	2.54	0.20	18	0.400, 0.417	444, 301	551
7	436, 412, 303	477, 452	2.74	0.70	16	0.396, 0.416	492, 451, 306	538
8	436, 412, 303	477, 452	2.74	0.75	16	0.395, 0.413	460, 274	522

[a] Solutions were made in DCM with a concentration of 0.1 mg/mL (polymers **1**–**6**) and 10^{-5} M (compounds **7** and **8**).
[b] Thin films were prepared by dropcasting concentrated solution of the compounds on quartz plate at room temperature.
[c] Bandgap, $E_g = hc/\lambda_{onset}$, where h = Plank's constant, c = velocity of light.
[d] Colour coordinates were measured using chromameter CS 100 A, calibrated with white light.

compounds showed bathochromic shifts, possibly due to close packing of polymer chains and molecules in the solid state [15,39,40].

3.4. Electrochemical properties

Electrochemical properties of the target compounds were investigated using cyclic voltammetry (Fig. 5). Acquired data are summarized in Table 3. Energy levels of highest occupied molecular orbitals (E_{HOMO}) were calculated from the half-wave potentials of oxidation peaks. Cyclic voltammograms of polymer **1**, **2**, **5**, **6** and model compounds **7**, **8** showed two irreversible oxidation peaks. Pyrene, being more electron rich compared to phenyl and fluorene moieties, acts as electron donor. Hence, the observed anodic peaks may be assigned to electrochemical oxidation of pyrene units [41]. For these compounds, reduction waves were not detectable within the scan range of −2 to +2 V. A completely different scenario was observed for polymers **3** and **4**, where, weak anodic peak was accompanied with strong cathodic peaks. It is conceivable that carbazole, being more electron rich compared to pyrene, donates electron to pyrene [42] and this leads to oxidation of carbazole and reduction of pyrene during the redox process. Both oxidation and reduction processes appeared to be irreversible in nature.

3.5. Self-assembly

Self-assembly of the synthesized compounds (**1**–**8**) were studied to obtain further insight about several interchain or intermolecular interactions. Toluene was selected as the solvent medium with the virtue of its high boiling point and solubilizing effect. Thin films of

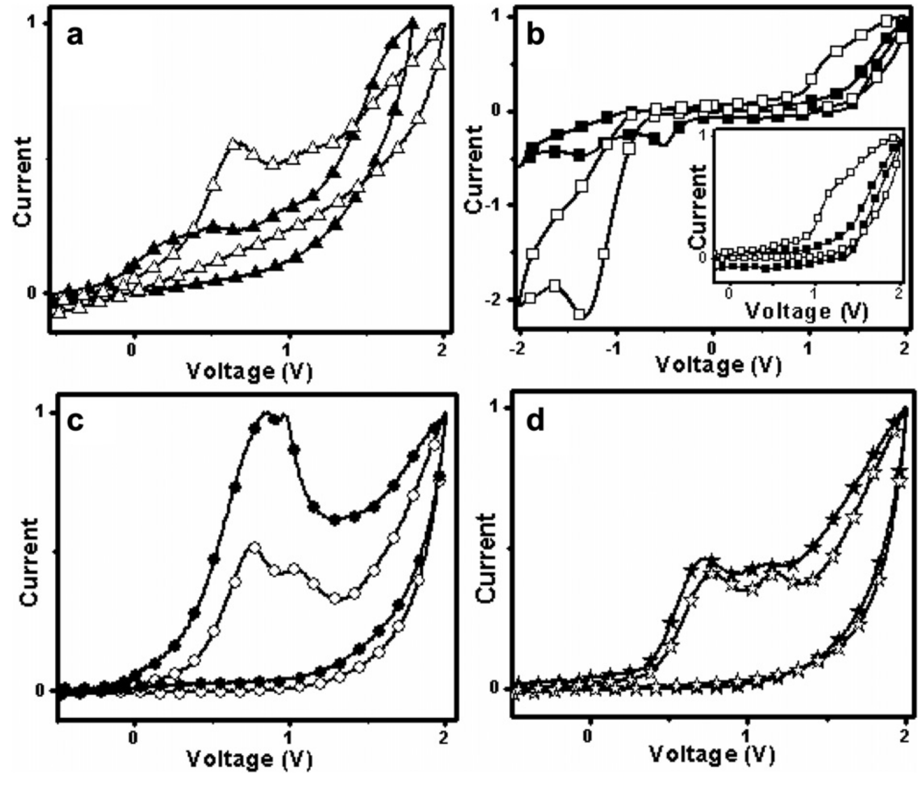

Fig. 5. Cyclic voltammograms of (a) **1** (▲) and **2** (△), (b) **3** (■) and **4** (□), (c) **5** (●) and **6** (○), (d) **7** (★) and **8** (☆). The data were collected at a scan rate of 100 mV s^{-1} using spin coated films (thickness ~50 nm) of the target compounds on ITO substrate and n-Bu_4NPF_6 in acetonitrile (0.1 M) as electrolyte.

Table 3
Electrochemical properties of the target compounds.

Compound	E_{ox}[a] (V)	$E_{ox}^{1/2}$[b] (V)	E_{HOMO}[c] (eV)	E_{red} (V)
1	0.44, 0.95	0.05	−4.35	
2	0.67, 1.14	0.42	−4.72	
3	0.24	0.12	−4.42	−0.51, −1.35
4	0.78, 1.19	0.57	−4.87	−1.33
5	0.79, 0.95	0.54	−4.84	
6	0.76, 1.05	0.56	−4.86	
7	0.72, 1.10	0.51	−4.81	
8	0.78, 1.17	0.56	−4.86	

[a] Peak value of the oxidation wave.
[b] Half-wave oxidation potential.
[c] $E_{HOMO} = -(4.3 + E_{ox}^{1/2})$ eV [43,44].

the target compounds were made by dropcasting 50 μL of the solution (0.2 mg/mL) on glass plate and allowing to slowly evaporate inside a desiccator. The SEM images of the dropcasted films of *cisoid*-polymers showed coiled fiber structure (Fig. 6 and Supplementary material Fig. S14), whereas, no well defined morphologies were found for the *transoid*-analogues and the model compounds. AFM image of similarly prepared film on ITO surface (Supplementary material Fig. S15) provided evidence for the thickness of the fiber as ∼50–200 nm.

4. Discussion

The results obtained from thermal, optical, electrochemical and self-assembly studies of the *cisoid*-, *transoid*-polymers and the model compounds suggest direct correlation between the shape of polymer backbone and physical properties. *Cisoid*-polymers (**1**, **3**, **5**) were found to be thermally more stable as compared to their *transoid*-analogues (**2**, **4**, **6**) (Table 1). Decomposition temperature corresponding to 5% weight loss (T_5, above 200 °C) was considered for the comparison purpose. A careful examination on the optical data revealed that absorption wavelength of *cisoid*-polymers is significantly red shifted as compared to their *transoid*-analogues. However, the model compounds (**7** and **8**) showed similar optical properties (Table 2). Results of cyclic voltammetry studies found E_{HOMO} of *cisoid*-polymers to be less negative as compared to *transoid*-polymers (Table 3). Although, the difference between model compounds is marginal.

The twisted backbone of *cisoid*-polymers forces the polymer chain to coil and facilitates intra- and interchain interactions between several non-adjacent units, which is not possible for the *transoid*-polymers with rigid rod backbone. Enhanced π-stacking between two non-adjacent pyrene in coil like *cisoid*-polymers is expected to show lower optical band gap. Similarly, higher thermal stability of *cisoid*-polymers can be attributed to the enhanced bond strength imparted by extra intra- and interchain interactions offered by coil morphology. The lower oxidation potentials of *cisoid*-polymers again can be attributed to the enhanced intra- and interchain interactions because, enhanced conjugation is known to result in lower oxidation potential [45]. SEM images of the dropcasted films of polymer solution (Fig. 6) showed coiled morphology of the *cisoid*-polymers.

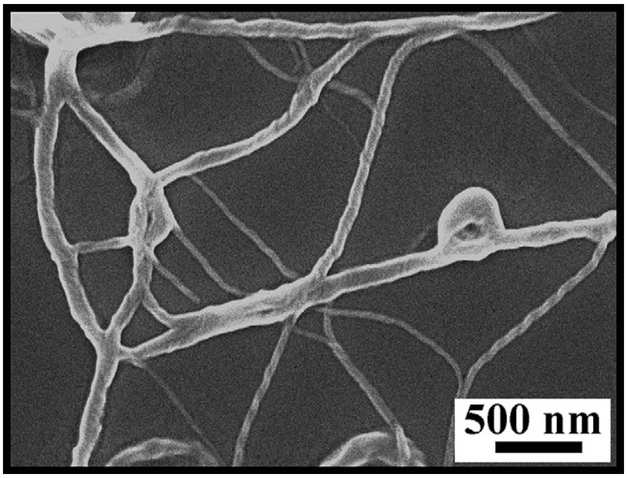

Fig. 6. SEM image of polymer **1** showed coiled fiber structure.

Similar optical properties of the model compounds (**7** and **8**) suggested similar π-conjugation through 1,8- and 1,6-linkages of pyrene and difference in physical properties between *cisoid*- and *transoid*-polymers could be due to the rigid shape of the polymer backbone. Lower optical band gap of polymers **1** and **2** compared to the corresponding model compounds (**7** and **8**) may be attributed to the extended conjugation over the polymer backbone or secondary interaction between several polymer chains.

The observed effect of spacer groups on optical properties can also be explained with respect to their role in controlling the shape of the polymer backbone. Comparison between polymers with different spacer groups (**1**, **2** and **3**, **4** and **5**, **6**) revealed the order of band gap, fluorene > carbazole > phenyl (for **1**, **3**, **5**) or carbazole > fluorene > phenyl (for **2**, **4**, **6**), which may be due to the overall shape of polymer backbone. The reason for phenyl spacer to show significant difference in optical properties between *cisoid*- and *transoid*-polymers (**1** and **2**) may be due to small size and rigid 1,4-linkage, which facilitates more effective interaction between two pyrenes in comparison with 3,6-disubstituted carbazole and 2,7-disubstituted fluorene.

The observed low band gap for the *cisoid*-polymers was in contrast with the results observed for homopolymer of *p*-phenyleneethynylene (P*p*PE, [16]) and copolymer of *p*-phenyleneethynylene and *m*-phenyleneethynylene (P*m*PE, [18]). Absorption wavelength of P*p*PE is known to be bathochromically shifted as compared to P*m*PE, which may be due to the lack of conjugation in 1,3-linkage of phenylene as compared to 1,4-linkages along the polymer backbone.

5. Conclusion

A new family of fluorescent conjugated polymers, poly(pyreneethynylene)s, have been synthesized by Sonogashira coupling of 1,8- or 1,6-diethynyl pyrene with dihaloderivatives of alkoxybenzene, carbazole and fluorene. The resultant polymers with differently shaped backbone were characterized using NMR, IR, MALDI-TOF and GPC. Detailed investigation about their optical, electrochemical and thermal properties revealed useful insight regarding structure–property relationship. Significant influence of shape of polymer backbone was found on the physical properties of the polymers. Kinked backbone of *cisoid*-polymers appeared to contribute towards lower band gap, less negative E_{HOMO} and higher thermal stability. A plausible explanation for such behaviour has been hypothesized with the formation of coil and rod structures by *cisoid*- and *transoid*-polymers, respectively. Added evidence of coiling of *cisoid*-polymers was obtained from SEM images of the dropcasted polymer films. Two model compounds were synthesized to check the extent of conjugation over 1,8- and 1,6-position of pyrene. The observed differences in physical properties between *cisoid*- and *transoid*-polymers is solely due to the shape of polymer backbone. These findings are significant as they enrich the conceptual knowledge required for designing performance specific polymers.

Acknowledgements

Authors acknowledge funding support from Agency for Science, Technology and Research (ASTAR), Singapore and technical support from Department of Chemistry, National University of Singapore. We also acknowledge the help and suggestions from Professor S. Sankararaman, Indian Institute of Technology Madras, India. JG thanks National University of Singapore and Ministry of Education, Singapore for a PhD scholarship.

Appendix. Supplementary material

Supplementary material associated with this article can be found in the online version, at doi:10.1016/j.polymer.2010.09.012.

References

[1] So F, Krummacher B, Mathai MK, Poplavskyy D, Choulis SA, Choong VE. J Appl Phys 2007;102:091101-1–091101-21.
[2] Kulkarni AP, Tonzola CJ, Babel A, Jenekhe SA. Chem Mater 2004;16(23):4556–73.
[3] Maillou T, Le Moigne J, Geffroy B, Lorin A, Rosilio A, Dumarcher V, et al. Synth Met 2001;124(1):87–9.
[4] Arias-Marin E, Arnault JC, Guillon D, Maillou T, Le Moigne J, Geffroy B, et al. Langmuir 2000;16(9):4309–18.
[5] Kraft A, Grimsdale AC, Holmes AB. Angew Chem Int Ed 1998;37(4):402–28.
[6] Bradley DDC. Curr Opin Solid State Mater 1996;1:789–98.
[7] Yang SH, Hsu CS. J Polym Sci Part A Polym Chem 2009;47(11):2713–33.
[8] Barik S, Valiyaveettil S. Macromolecules 2008;4(17):6376–86.
[9] Ravindranath R, Ajikumar PK, Bahulayan S, Nurmawati MH, Akira B, Advincula RC, et al. J Phys Chem B 2007;111(23):6336–43.
[10] Tour JM. J Org Chem 2007;72(20):7477–96.
[11] Forrest SR. Nature 2004;428(6986):911–8.
[12] Fan LJ, Zhang Y, Murphy CB, Angell SE, Parker MFL, Flynn BR, et al. Coord Chem Rev 2009;253(3–4):410–22.
[13] Thomas SW, Joly GD, Swager TM. Chem Rev 2007;107(4):1339–86.
[14] McGehee MD, Heeger AJ. Adv Mater 2000;12(22):1655–68.
[15] Bunz UHF. Chem Rev 2000;100(4):1605–44.
[16] Li H, Powell DR, Hayashi RK, West R. Macromolecules 1998;31(1):52–8.
[17] Chu Q, Pang Y. Macromolecules 2002;35(20):7569–74.
[18] Pang Y, Li J, Bin H, Karasz FE. Macromolecules 1998;31(19):6730–2.
[19] Pang Y, Li J, Barton TJ. J Mater Chem 1998;8(8):1687–90.
[20] Karim SMA, Musikabhumma K, Nomura R, Masuda T. Proc Jpn Acad Ser B 1999;75(5):97–100.
[21] Rivera E, Wang R, Zhu XX, Zargarian D, Giasson R. Polymer 2002;43(19):5059–68.
[22] Rivera E, Wang R, Zhu XX, Zargarian D, Giasson R. J Mol Catal A 2003;204–205:325–32.
[23] Mikroyannidis JA. Synth Met 2005;155(1):125–9.
[24] Shimizu H, Fujimoto K, Furusyo M, Maeda H, Nanai Y, Mizuno K, et al. J Org Chem 2007;72(4):1530–3.
[25] Qu L, Shi G. Chem Commun 2004;24:2800–1.
[26] http://www.jobinyvon.com/SiteResources/Data/MediaArchive/files/Fluorescence/applications/quantumyieldstrad.pdf.
[27] Li GR, Wang X, Wang F. Tetrahedron Lett 2006;47(5):723–5.
[28] Swager TM, Gil CJ, Wrighton MS. J Phys Chem 1995;99(14):4886–93.
[29] Huang SP, Huang GS, Chen SA. Synth Met 2007;157(21):863–71.
[30] Zhang Z, Ma Z, Xie S, Zheng Z, Xiao X, Wei W, et al. J Mater Sci 2006;41(10):3159–62.
[31] Maeda H, Maeda T, Mizuno K, Fujimoto K, Shimizu H, Inouye M. Chem Eur J 2006;12(3):824–31.
[32] Lhez SL, Fages F. Eur J Org Chem 2005;2005(13):2684–8.
[33] Ji S, Yang J, Yang Q, Liu S, Chen M, Zhao J. J Org Chem 2009;74(13):4855–65.
[34] Hong JM, Cho HN, Kim DY, Kim CY. Synth Met 1999;102(1-3):933–4.
[35] Sienkowska MJ, Monobe H, Kaszynski P, Shimizu Y. J Mater Chem 2007;17(14):1392–8.
[36] Kalyansundaram K, Thomas JK. J Am Chem Soc 1977;99(7):2039–44.
[37] Bredas JL, Cornil J, Heeger AJ. Adv Mater 1996;8(5):447–52.
[38] Zhang L, Zhang QY, Yan H, Zhang JP, Gu JW, Zhang HP, et al. Synth Met 2009;159(19–20):2038–42.
[39] Jenekhe SA, Osaheni JA. Science 1994;265(5173):765–8.
[40] Wang S, Wu P, Han Z. Macromolecules 2003;36(12):4567–76.
[41] Zotti G, Schiavon G. Synth Met 1992;47(2):193–202.
[42] Zhao Z, Xu X, Wang H, Lu P, Yu G, Liu Y. J Org Chem 2008;73(2):594–602.
[43] Simon J, Andre JJ. Molecular semiconductors. Berlin, Germany, Heidelberg: Springer-Verlag; 1985. p. 98.
[44] Loutfy RO, Cheng YC. J Chem Phys 1980;73(6):2902–10.
[45] Hagberg DP, Marinado T, Karlsson KM, Nonomura K, Qin P, Boschloo G, et al. J Org Chem 2007;72(25):9550–6.